

## Electron transfer to $n \geq 3$ states of fluorine following $K$ - plus $L$ -shell ionization by heavy ions

O. Benka,\* R. L. Watson, B. Bandong, and K. Parthasaradhi†

Cyclotron Institute and Department of Chemistry, Texas A&M University, College Station, Texas 77843

(Received 15 August 1983)

The energies of fluorine  $K\alpha$  x-ray satellite and hypersatellite peaks appearing in spectra for solid alkali and alkaline-earth fluorides and for gaseous HF have been compared. The energies for the solid compounds were found to be systematically lower than those for the gas. Spectra excited in thick solid targets by 80-MeV Ar ions exhibit new series of peaks located in the energy region just above the  $K\alpha$  hypersatellites. These peaks have been attributed to  $K\beta$  hypersatellite transitions from levels having  $n \geq 3$ . Both the energy deviations and the presence of  $K\beta$  hypersatellites indicate that electron transfer to  $n \geq 3$  levels occurs in the solids prior to  $K$  x-ray emission. A mechanism for the electron transfer process is proposed and support for this mechanism is provided by a simple classical model.

### I. INTRODUCTION

A series of investigations of the effects of chemical environment on the ion-excited  $K$  x-ray spectrum of fluorine have recently been reported.<sup>1-4</sup> In this previous work, spectra of the alkali and alkaline-earth fluorides were measured using 5.5-MeV He, 22-MeV C, 48-MeV Mg, and 80-MeV Ar ions. In addition, measurements were performed on neon to establish the primary  $L$ -vacancy distribution produced by each projectile in  $K$ -shell ionizing collisions,<sup>5</sup> and on a variety of fluorine bearing gases to study the properties of interatomic electron transfer in single molecules.<sup>4</sup>

The spectra obtained with He ions provided evidence for a resonant electron transfer (RET) mechanism<sup>1</sup> in which an electron is transferred from an outer  $np$  level of a neighboring metal ion to the  $2p$  level of a fluorine ion following  $1s2p$  ionization of  $F^-$ . As the primary state of ionization was increased through the use of higher  $Z$  projectiles, rapid electron transfer to the fluorine  $L$  shell was found to occur largely via a mechanism that (unlike RET) does not appear to involve  $L$  shell level matching.

Detailed analyses of the intensity distributions of the  $K\alpha$  satellites and hypersatellites enabled the determination of rate constants for  $L$ -vacancy filling.<sup>2,4</sup> A single rate constant of about  $30 \times 10^{-4}$  a.u. was found to characterize both the  $K\alpha$  satellite and hypersatellite intensity distributions for the solid compounds reasonably well, whereas the rate constants for the gaseous compounds were significantly smaller. In solid compounds, it was found that electron transfer to the fluorine  $L$  shell prior to  $K$ -vacancy decay occurs with a probability of the order of 95% for highly ionized states, such as  $KL$ .<sup>6</sup>

The nondiscriminating nature of the  $L$ -vacancy filling process for highly ionized ions produced with heavy-ion projectiles and the differences observed for solids and gases suggested a two-step mechanism analogous to that observed for electron capture by highly stripped recoil ions in gas targets.<sup>6</sup> It was proposed that the rapid

transfer of electrons selectively occurs to states of the fluorine ion which match the energies of bound states in the surrounding neutral atoms of the solid.<sup>4</sup> Because of the high degree of  $K$ - plus  $L$ -shell ionization produced in heavy ion collisions, electron transfer would presumably proceed to states having  $n \geq 3$ , and subsequent Auger decay to the  $L$  shell would be required to account for the filling of  $L$  vacancies. While available information on Auger decay rates for singly ionized atoms indicates that these transitions are probably sufficiently fast to make this two-step mechanism plausible, detailed calculations for highly ionized atoms will be required to test this hypothesis further.

On the other hand, the first step in the  $L$ -shell filling process is amenable to experimental verification. The purpose of the present work was twofold, (a) to examine the energies of the fluorine  $K\alpha$  satellites and hypersatellites in spectra excited by Mg and Ar ions for evidence of energy shifts indicative of the presence of electrons in  $n \geq 3$  levels, and (b) to search the region of the fluorine  $K$  x-ray spectrum above the  $K\alpha$  hypersatellites for evidence of  $K\beta$  hypersatellite transitions.

### II. EXPERIMENTAL METHODS

The spectral measurements were performed with a Johansson-type spectrometer having a 12.7-cm focal circle radius and a curved thallium acid phthalate (TAP) crystal. A beam of 80-MeV  $Ar^{5+}$  ions from the Texas A&M variable energy cyclotron was directed onto thick targets of LiF, NaF, KF,  $MgF_2$ , and  $CaF_2$  and high statistics scans were carried out over the  $K\alpha$  and  $K\beta$  hypersatellite regions (750–1000 eV). The targets were made by pressing the appropriate powdered materials into pellets having dimensions of 1.27 cm diameter and 3 mm thickness.

The energies reported herein for the  $K\alpha$  satellites were obtained from an analysis of spectra taken in a prior study using 80-MeV Ar ions incident on thin targets.<sup>4</sup> The use of thin targets avoided spectral distortions associated with the fluorine  $K$  absorption edge. Energies for gaseous HF

were likewise obtained from an analysis of spectra taken in the above-mentioned study using 48-MeV Mg ions. Accurate peak centroids were extracted in each case by means of a least-squares peak fitting program (FACELIFT).

Spectrometer energy calibrations were performed during each of the runs in which the various fluorine target spectra were measured. In general, the calibration procedure involved recording the  $KL^0$  peak positions of Na (in NaF), measured in both first and second order, F (in NaF), and Ne. The energies of the  $KL^0$  peaks were assumed to be those listed in the well-known compilation of Bearden.<sup>7</sup> Based upon the linearity of the calibration curves (wavelength versus spectrometer odometer reading), the uncertainty in the energy calibration is estimated to be  $\pm 0.3$  eV.

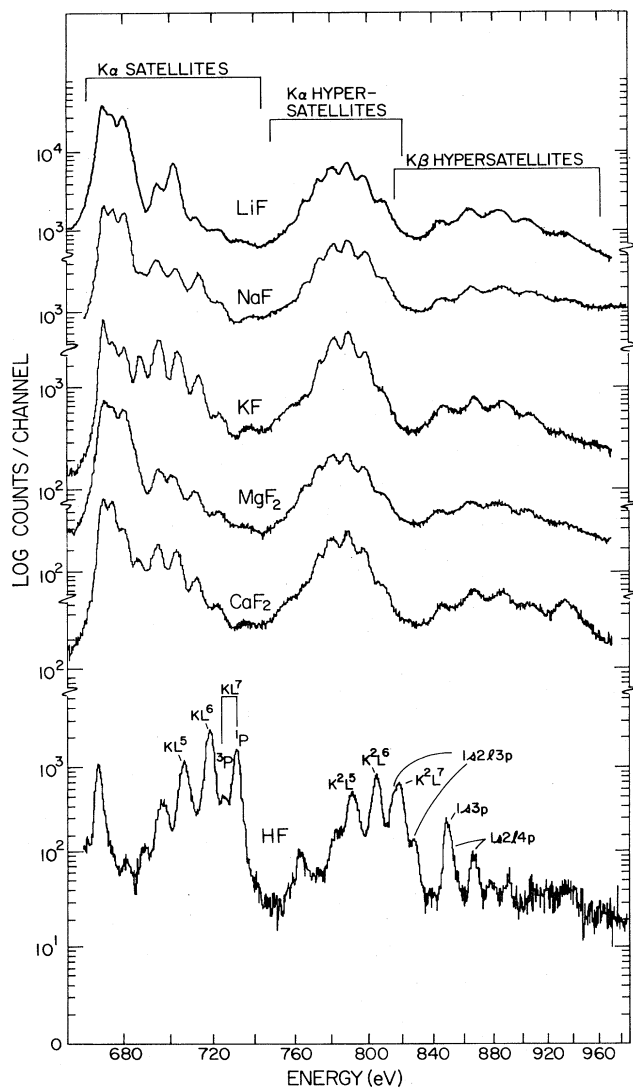


FIG. 1. Comparison of the spectra of fluorine  $K$  x-rays excited in thick solid targets of alkali and alkaline-earth fluorides by 80-MeV Ar ions and in gaseous HF by 48-MeV Mg ions.

### III. RESULTS

Shown in Fig. 1 is a comparison of the fluorine spectra for the solid targets, excited by 80-MeV Ar ions, with the spectrum of (gaseous) HF obtained using 48-MeV Mg ions. The peaks extending over the energy region 677–738 eV are the  $K\alpha$  satellites and the peaks extending over the energy region 761–828 eV are the  $K\alpha$  hypersatellites. A new feature appearing in the spectra for the solid targets, and one which is absent in the HF spectrum, is the broad series of peaks spanning the energy region 820–970 eV. For reasons which will be explained in Sec. IV, these peaks have been attributed to  $K\beta$  hypersatellites associated with  $np-1s$  transitions in which  $n \geq 3$ .

Listed in Table I are the experimental  $K\alpha$  satellite and hypersatellite energies determined for the solid compounds and for gaseous HF. Within experimental error, which is estimated to be  $\pm 0.5$  eV, all of the solid compounds gave the same energies. As may be seen from Table I, the energies obtained for HF are systematically larger than those for the solid targets and the deviation increases steadily as the number of  $L$  vacancies increases. This trend is shown graphically in Fig. 2 where the energy differences  $E(\text{HF})-E(\text{solid})$  are plotted versus the number of  $L$  vacancies.

The experimental energies of the peaks labeled  $K\beta$  hypersatellites in Fig. 1 are listed in Table II. Considerable variation of these peak energies occurs among the various compounds, and for this reason energies are listed separately for each compound. Because of the large uncertainties associated with the low intensity first and last peaks of the series ( $B1$  and  $B7$  in Table II), only average energies are given for them.

TABLE I. Experimental fluorine  $K\alpha$  x-ray energies (eV) for (solid) alkali and alkaline-earth fluorides and (gaseous) HF.

Peak	Solids	HF
<i>K<math>\alpha</math> satellites</i>		
$KL^0$	676.8 <sup>a</sup>	
$KL^1$	680.5	
$KL^2$	685.5	
$KL^3$	692.1	
$KL^4$	699.9	702.7
$KL^5$	708.5	712.8
$KL^6$	717.9	724.4
$KL^7(^3P)$		731.7
$KL^7(^1P)$	728.7	737.5
<i>K<math>\alpha</math> hypersatellites</i>		
$K^2L^0$	761.2	
$K^2L^1$	764.9	
$K^2L^2$	771.8	
$K^2L^3$	779.3	
$K^2L^4$	787.3	789.2
$K^2L^5$	796.1	799.4
$K^2L^6$	805.3	813.1
$K^2L^7$	816.5	827.8

<sup>a</sup>Calibration energy from Ref. 7.

TABLE II. Experimental energies for the  $K\beta$  hypersatellite peaks (eV).

Peak	LiF	NaF	KF	MgF <sub>2</sub>	CaF <sub>2</sub>	Average
B1						833 ± 5
B2	853.5	853.4	855.9	852.6	856.0	854.3 ± 1.6
B3	872.4	873.2	876.3	872.5	879.5	874.0 ± 1.8
B4	893.2	894.2	896.9	892.9	894.9	894.4 ± 1.6
B5	914.7	917.4	917.2	915.1	916.5	916.2 ± 1.2
B6	935.9	943.5	938.9	938.1	943.7	940.6 ± 2.7
B7						959 ± 5

As indicated above, the  $K\beta$  hypersatellite peaks are much broader than the  $K\alpha$  satellite and hypersatellite peaks. The average peak widths [full width at half maximum (FWHM)], including instrumental contributions, were 5.0, 7.2, and 17.1 eV, respectively for the  $K\alpha$  satellites, the  $K\alpha$  hypersatellites, and the  $K\beta$  hypersatellites. The instrumental resolution varied from 3.3 eV for  $KL^0$  to 6.3 eV for peak B7. Relative intensities (corrected for absorption and reflectivity) are listed in Table III for the  $K\alpha$  and  $K\beta$  hypersatellites.

The drastic changes in the intensity distributions of the  $K\alpha$  satellites and hypersatellites observed in going from the solids to HF gas (see Fig. 1) reflect the importance of electron transfer to the  $L$  shell prior to  $K$  x-ray emission in the solid-state environment.<sup>4</sup> The point of particular interest in the present work is the fact that the  $K\beta$  hypersatellite peaks are not present in the HF spectrum. The energies of the few peaks which do appear in the energy region above 820 eV correspond quite well to those predicted by Dirac-Fock calculations<sup>8</sup> for transitions of

the type  $1s2lnp-1s^2l$  and  $1snp-1s^2$ . Numerical results pertaining to these transitions are presented in Table IV.

## IV. DISCUSSION

### A. $K\alpha$ satellite and hypersatellite energy shifts

In attempting to understand the origin of the energy differences observed between the solid compounds and HF gas, it is desirable to compare the experimental  $K\alpha$  transition energies with those predicted by free-ion calculations. An absolute comparison of the measured satellite and hypersatellite energies with the energies predicted by Hartree-Fock or Dirac-Fock calculations is complicated by the fact that the experimental energies are averages of the energies of the many multiplet transitions which comprise each satellite and hypersatellite group. In order to calculate properly averaged theoretical energies, each multiplet transition energy must be computed and its relative intensity estimated from theoretical fluorescence yields and initial-state population probabilities. This laborious procedure was recently carried out for neon and the calculated average energies agreed to within 0.5 eV for the satellites and to within 1.7 eV for the hypersatellites, on average.<sup>5</sup> For the present purposes, it is sufficient to make a relative comparison between the corresponding energies of fluorine and neon. This procedure is advantageous because all relative energies, whether they are computed from individual multiplet term energies or from average-of-configurations energies, lie along a single smooth curve. Such a comparison is shown for the  $K\alpha$  satellites in Fig. 3(a) and for the  $K\alpha$  hypersatellites in Fig. 3(b). The solid squares in these figures are plotted at the intersection points of corresponding fluorine and neon multiplet transition energies computed using the Hartree-Fock program of Fischer.<sup>11</sup> The solid line was constructed by drawing a smooth curve through the intersection points of corresponding fluorine and neon transition energies computed from average-of-configurations initial- and final-state energies.

The above comparison indicates that as long as the fluorine and neon energies are averaged in the same way, their relative energies should lie along the smooth curves in Fig. 3. The experimental energies are shown in Fig. 3 by the open circles for the solid fluorine compounds and the open squares for HF. It is apparent that the HF energies agree very well with the Hartree-Fock values. There-

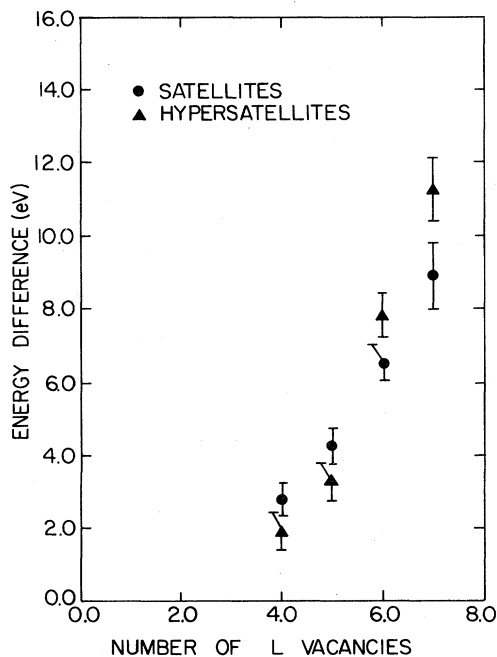


FIG. 2. Gas (HF)/solid energy differences [ $E(\text{HF})-E(\text{solid})$ ] between corresponding satellite and hypersatellite peaks.

TABLE III. Relative peak areas of the  $K\alpha$  and  $K\beta$  hypersatellites appearing in the spectra of the solid fluorine compounds.

Peak	LiF	NaF	KF	MgF <sub>2</sub>	CaF <sub>2</sub>
$K^2L^0$	48	34	33	28	29
$K^2L^1$	153	98	81	85	63
$K^2L^2$	676	331	110	227	101
$K^2L^3$	897	790	363	429	241
$K^2L^4$	2043	1831	868	879	577
$K^2L^5$	1792	1753	881	747	539
$K^2L^6$	1372	1279	557	488	376
$K^2L^7$	721	664	200	295	158
$B1$	15	65	47	48	21
$B2$	283	175	151	140	78
$B3$	546	331	194	186	145
$B4$	512	408	168	204	119
$B5$	298	237	85	100	96
$B6$	167	121	31	64	76
$B7$	74	18	13	18	17

fore, it must be concluded that the energies for the solid compounds are lowered by some effect associated with the solid-state environment.

The most likely cause of the observed energy shifts in the solid compounds is screening arising from the presence of electrons in outer ( $n > 2$ ) energy levels. Since the  $L$  shell is the outermost shell of a ground-state  $F^-$  ion, such electrons are normally unbound. Following  $K$ - plus  $L$ -shell ionization, however, the  $n \geq 3$  states drop out of the continuum and can accommodate bound electrons. To

test this hypothesis, the average energies of the initial- and final-state configurations were calculated for the various satellite and hypersatellite configurations in the presence of one to four  $M$ -shell ( $3p$ ) electrons. The fluorine transition energies are plotted versus the corresponding energies for neon (without  $3p$  electrons) in Fig. 4. Also shown are the experimental energies for HF gas and the solid fluorine compounds, as in Fig. 3. It may be seen that the  $K\alpha$  satellite energies for the solid compounds all line up closely with the curve corresponding to three  $M$ -shell elec-

TABLE IV. Experimental and theoretical transition energies for few-electron fluorine ions (eV).

Transition	Experiment		Dirac-Fock <sup>a</sup>
$2p-1s$	827.8		827.7 (827.4) <sup>b</sup>
$3p-1s$			980.7
$4p-1s$			1034.3
$1s 2p(^3P)-1s^2$	731.7		730.4 (731.6) <sup>c</sup>
$1s 2p(^1P)-1s^2$	737.5		736.8 (737.8) <sup>c</sup>
$1s 3p(^1P)-1s^2$	857.6		856.4
$1s 4p(^1P)-1s^2$			898.5
$1s 5p(^1P)-1s^2$			918.0
$1s 2l 3p-1s^2 2l$	823.0	( $l=p$ )	{ 823.8
			{ 829.8
	836.1	( $l=s$ )	{ 829.4
			{ 838.6
$1s 2l 4p-1s^2 2l$	863.8	( $l=p$ )	{ 858.4
			{ 864.5
	875.7	( $l=s$ )	{ 864.2
			{ 873.8

<sup>a</sup>Calculated using the computer code of Desclaux (Ref. 8).

<sup>b</sup>From Ref. 9.

<sup>c</sup>From Ref. 10.

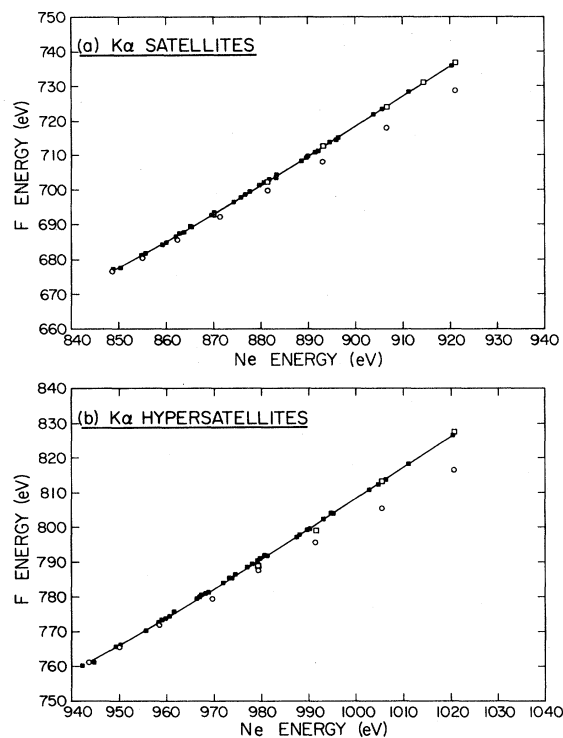


FIG. 3. Calculated multiplet transition energies (solid squares) and average-of-configurations transition energies (solid line) for fluorine plotted against the corresponding values for neon. The open circles show the experimental values for the solid fluorides and the open squares show the experimental values for HF gas.

trons. The  $K\alpha$  hypersatellite energies correspond most closely with the  $m=4$  line. Hence the observed energy deviations for the solid fluorine compounds are consistent with the shifts expected as a result of the presence of three to four  $M$ -shell electrons at the time of  $K$ -vacancy decay.

### B. $K\beta$ hypersatellites

The assignment of the peaks labeled  $B1$  through  $B7$  (see Table II) to  $K\beta$  hypersatellite transitions is made plausible by the above evidence that  $M$ -shell electrons are present at the time of  $K\alpha$  x-ray emission. This identifica-

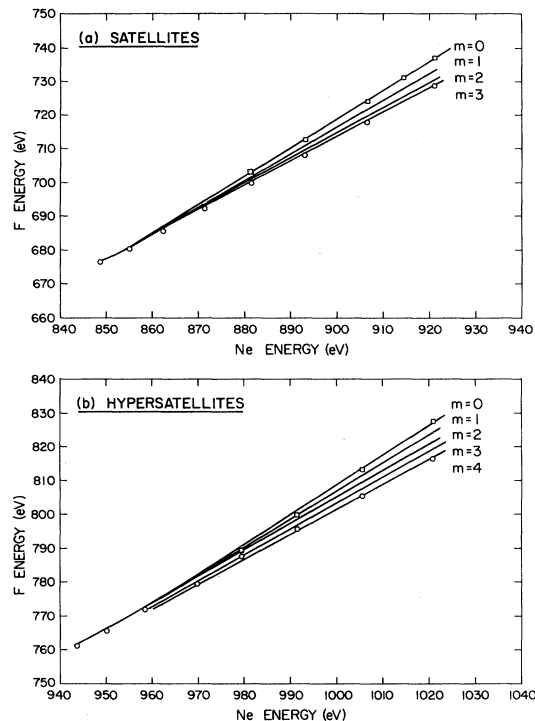


FIG. 4. Calculated average-of-configurations transition energies for fluorine ions containing  $m$  electrons in  $3p$  levels plotted against the corresponding values for neon (without  $3p$  electrons). The open circles show the experimental values for the solid fluorides and the open squares show the experimental values for HF gas.

tion can be further substantiated by comparing the transition energies and intensities with theoretical predictions.

In Table V are listed  $3p-1s$  transition energies calculated from Hartree-Fock average-of-configurations initial- and final-state energies. The value of  $m$  in this table indicates the number of  $3p$  electrons present in the initial-state configuration. Comparison of these energies (which are not expected to be accurate to better than  $\pm 5$  eV) with the experimental energies given in Table II leads to the assignments listed in Table VI. The peak  $B7$  is attributed to transitions from the  $N$  shell. In fact, the unusually large widths of the  $K\beta$  hypersatellite peaks suggest that they

TABLE V. Hartree-Fock  $3p-1s$  transition energies (eV) for fluorine atoms having initial states with one to four electrons in  $3p$  levels.

Inner-shell vacancy configuration	Number of $M$ -shell electrons present			
	$m=1$	$m=2$	$m=3$	$m=4$
$K^2L^2$	816	815	813	812
$K^2L^3$	837	834	831	830
$K^2L^4$	861	856	853	850
$K^2L^5$	887	881	879	873
$K^2L^6$	915	907	906	899
$K^2L^7$	946	941	933	927
$K^2L^8$	980	971	964	957

TABLE VI. Predicted electron configurations for the observed  $K\beta$  hypersatellite peaks.

Peak	Number of electrons present	
	$L$ shell	$M$ shell
$B1$	5	2-3
$B2$	4	2-3
$B3$	3	3-4
$B4$	2	4-5
$B5$	1	5
$B6$	0	5-6
$B7$	0	

may all contain overlapping contributions from  $N$ -shell and possibly higher transitions.

It naturally follows that if  $K\beta$  hypersatellites are present in the spectra of the solid compounds, there should also be evidence of  $K\beta$  satellite transitions. Unfortunately, the  $K\beta$  satellites lie, for the most part, within the  $K\alpha$  hypersatellite region. The peak at around 730 eV in Fig. 1 is probably due to one of the lower-energy  $K\beta$  satellites.

Additional support for the hypothesis that the peaks  $B1$  to  $B7$  arise from  $np-1s$  transitions, where  $n \geq 3$ , is provided by a comparison of their intensities with the intensities of the  $K\alpha$  hypersatellite peaks for the corresponding  $L$ -vacancy configurations (see Table III). The ratios of the  $K\beta$  to  $K\alpha$  hypersatellite intensities may be compared with those predicted by the semiempirical scaling law:

$$R(\beta/\alpha) \approx \frac{N(n'l'')}{N(n'l')} \left[ \frac{Z_{\text{eff}}(n'l'')}{Z_{\text{eff}}(n'l')} \right]^2 \frac{T(n'l'' \rightarrow nl)}{T(n'l' \rightarrow nl)}$$

In the above equation  $R(\beta/\alpha)$  is the ratio of the  $K\beta$  hypersatellite intensity to the corresponding  $K\alpha$  hypersatellite intensity,  $N(nl)$  is the number of electrons in the level from which the transition occurs,  $Z_{\text{eff}}(nl)$  is the screened atomic number for the level from which the transition occurs as calculated from Slater's rules,<sup>12</sup> and  $T(n'l' \rightarrow nl)$  is the theoretical hydrogen atom transition probability from level  $n'l'$  to  $nl$  (from Ref. 13). As is shown in Ref. 14, this scaling law yields values which, in general, agree with theoretical transition probability ratios to better than 20%.

The results are shown in Fig. 5. The solid curves are drawn through the values of the  $3p-1s/2p-1s$  transition intensity ratios calculated with the above equation for a  $3p$  electron population ranging from 1 to 5. The value of  $l$  indicates the number of  $L$  electrons present, which are assumed to be statistically distributed between the  $2s$  and  $2p$  levels. Along the right side of Fig. 5 are plotted the experimental values obtained using the peak assignments deduced from the peak energies (as given in Table VI). The filled circles show the averages and the error bars show the ranges of the ratios for all the solid compounds. It is apparent that, overall, the experimental ratios are fairly consistent with those expected for  $3p$  electron populations of 2-5, and are therefore in general agreement with the conclusions reached in the peak energy comparison. It should be noted, however, that the experimental average

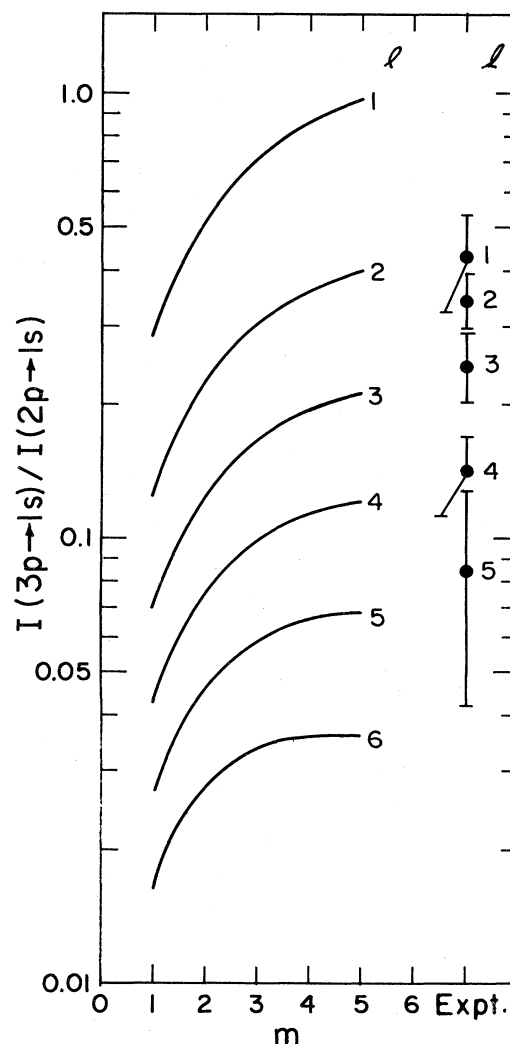


FIG. 5. Comparison of the predicted  $(3p-1s)/(2p-1s)$  intensity ratios with those determined from the spectra. The values of  $m$  indicate the numbers of  $L$ - and  $M$ -shell electrons assumed to be present.

intensity ratios correspond to decreasing numbers of  $M$  electrons as  $l$  decreases, with the ratio for  $l=1$  falling conspicuously low. A possible explanation for this trend might be that as  $l$  decreases (i.e., as the degree of inner-shell ionization increases), the electron transfer process begins to shift from the  $M$  shell to the  $N$  shell, thereby reducing the number of  $M$ -shell electrons available to participate in a  $K\beta$  transition. Thus a reduction in the number of  $M$  electrons would account for the lowering of the intensity ratios of the peaks for  $l=2$  and 1 while the addition of electrons to the  $N$  shell would maintain the degree of screening necessary to account for the peak energy. Transitions from the  $N$  shell would have higher energies and would presumably contribute primarily to peaks  $B5$ ,  $B6$ , and  $B7$ . In fact, as was pointed out above, peak  $B7$  must arise entirely from  $n \geq 4$  transitions.

### C. Electron transfer mechanism

The evidence presented above indicates that electrons from surrounding atoms in a solid transfer to  $n \geq 3$  states of the highly ionized fluorine atom, produced in the collision, on a time scale comparable to the  $K$ -vacancy lifetime ( $\sim 10^{-13}$  sec). A possible mechanism for this transfer process is one analogous to that proposed for selective electron capture into high  $n$  states of highly stripped, slowly recoiling ions undergoing secondary collisions with free atoms in a gas target.<sup>6</sup> In this case, the transfer of electrons selectively occurs to states of the ion which match the energies of bound states in the neutral atom collision partner. As the ion approaches the neutral atom, the potential barrier between the two partners decreases below the energies of the outer electrons of the neutral atom and allows electrons to transfer to energy matched states of the ion.

In the present case of an ionic solid, the internuclear separation  $R$  between the fluorine ion and the neighboring metal ions is essentially fixed. The situation before and after the collision is depicted schematically for an alkali fluoride in Fig. 6. Before the collision [Fig. 6(a)], the outer  $np$  levels of the  $M^+$  ions and the  $2p$  levels of the  $F^-$  ions are isolated within their own potential wells. As a result of a heavy-ion collision, a highly charged  $F^{q+}$  ion is produced. The charge  $q+$  on the fluorine ion causes the  $n > 2$  states to drop out of the continuum and also lowers the potential barrier between adjacent  $F^{q+}/M^+$  ion pairs, as shown in Fig. 6(b). If the barrier drops below the energy of the  $M^+$  ion  $np$  states, electrons are free to pass over to near-lying states of the  $F^{q+}$  ion.

The above picture may be tested using a simple classical model similar to the one employed by Mann *et al.*<sup>6</sup> Two conditions must be satisfied in order for rapid electron transfer to occur:

$$E_M \simeq E_F, \quad (1a)$$

$$E_M \geq U_m. \quad (1b)$$

In the above,  $E_M$  is the energy of the outermost occupied level of the metal ion,  $E_F$  is the energy of the level in the fluorine ion to which an electron is to be transferred, and

$U_m$  is the maximum energy of the potential barrier. The energy  $E_M$  may be expressed as

$$E_M = -E_M^{\text{FI}}(np) + E_M^\alpha - \frac{(q+1)e^2}{R}, \quad (2)$$

where  $E_M^{\text{FI}}(np)$  is the outer  $np$  free-ion binding energy,  $E_M^\alpha$  is the Madelung energy for the metal ion, and the term  $(q+1)e^2/R$  accounts for the additional Coulomb energy due to the adjacent  $q+$  fluorine ion. Similarly, the energy  $E_F$  is given by

$$E_F = -E_F^{\text{FI}}(n) - E_F^\alpha - e^2/R, \quad (3)$$

where  $E_F^{\text{FI}}(n)$  is the free-ion binding energy of the state to which the electron is transferred,  $E_F^\alpha$  is the Madelung energy of an  $F^-$  ion, and  $e^2/R$  is the Coulomb energy resulting from the additional positive charge on the adjacent metal ion after the electron has been transferred. For high charge states, the fluorine free-ion binding energy may be approximated by

$$E_F^{\text{FI}}(n) \simeq 13.6q^2/n^2. \quad (4)$$

The barrier potential is approximately given by

$$U = \frac{-ae^2}{r} - \frac{qe^2}{R-r}, \quad (5)$$

where  $r$  is the distance from the metal ion, which has charge  $a$  ( $a=2$  for the alkali-metal ions and 3 for the alkaline-earth ions). The maximum barrier energy is obtained from Eq. (5),

$$U_m = \frac{-e^2(\sqrt{a} + \sqrt{q})^2}{R}. \quad (6)$$

The energies  $E_M$ ,  $E_F$ , and  $U_m$  were calculated for NaF, KF, MgF<sub>2</sub>, and CaF<sub>2</sub> using values of  $E_M^{\text{FI}}(np)$  from Ref. 15 and Madelung energies which, for NaF and KF were calculated using the Madelung constants and  $R$  values given by Tosi,<sup>16</sup> and for MgF<sub>2</sub> and CaF<sub>2</sub> were obtained from Ref. 17. These energies are compared in Fig. 7 for  $q=9, 8, 7,$  and  $6$ . The dashed lines indicate the  $E_F$  energy positions for the specified values of  $n$ . For each of the compounds, the results show that the energies of the metal-ion  $np$  levels are above the maximum barrier ener-

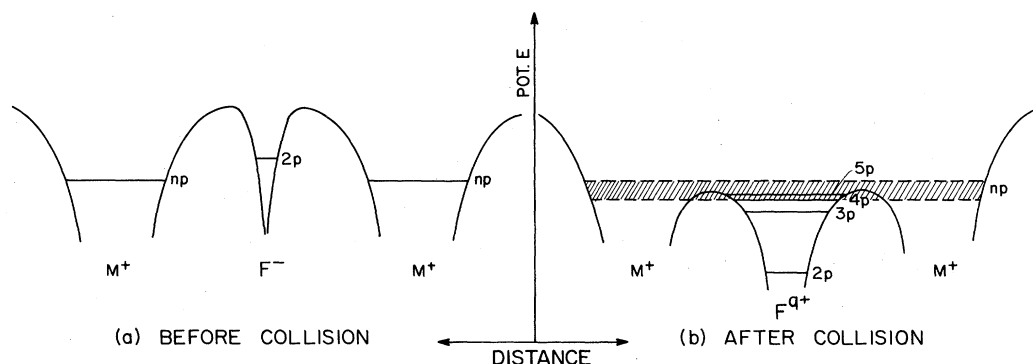


FIG. 6. Potential energy diagrams for an alkali fluoride crystal before and after a heavy-ion collision, illustrating the proposed electron transfer mechanism.

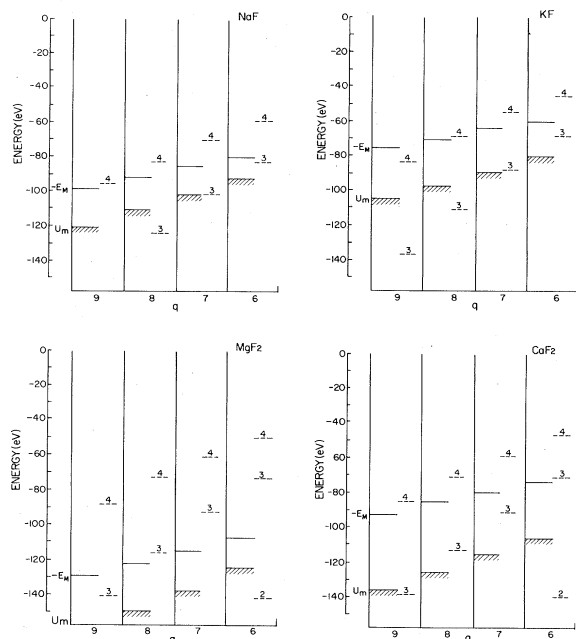


FIG. 7. Comparison of the energies  $E_M$ ,  $U_m$ , and  $E_F$  predicted by the simple classical model for different fluorine ion charges. The  $E_F$  are shown by the dashed lines for the values of  $n$  indicated.

gies and that the fluorine ion energies which most closely match are those for  $n=3$  and 4.

Quantum-mechanical effects, of course, are not taken into account by this simple classical treatment. A more realistic model must view the system as a molecular complex. In the case of NaF, for example, the crystal structure is face-centered cubic. This means that each fluorine ion is surrounded by six nearest-neighbor sodium ions. Following a heavy-ion collision in which a charge of  $q+$  is created at a fluorine site, a molecular complex  $[\text{Na}_6\text{F}]^{q+6}$  is formed and the 36  $2p$  electrons of the sodium ions must settle into molecular orbitals which extend over the whole complex. In this model, the intensities of the  $np$ - $1s$  fluorine transitions must reflect the molecular orbital electron density in the vicinity of the fluorine site.

## V. CONCLUSIONS

Comparisons of the spectra of fluorine  $K$  x rays excited by 2-MeV/amu Mg and Ar ions in solid alkali and

alkaline-earth fluorides with the spectrum obtained for gaseous HF have revealed that the solid target  $K\alpha$  satellite and hypersatellite energies are lower than those expected for free ions. In addition, a broad series of peaks have been observed in the solid target spectra appearing just above the  $K\alpha$  hypersatellite energy region. These peaks have been attributed to  $np$ - $1s$  transitions from levels having  $n \geq 3$  on the basis of transition energy and relative intensity considerations. The same considerations indicate that a substantial number of electrons are present in these levels at the time of  $K$  x-ray emission.

The fact that the  $K\alpha$  satellite and hypersatellite energies observed for HF are not shifted relative to the free-ion energies and the  $K\beta$  hypersatellite structure is absent in the HF spectrum indicates that similar populations of  $n \geq 3$  levels are not produced in heavy-ion collisions with free  $\text{F}^-$  ions. It is concluded, therefore, that the electrons residing in  $n \geq 3$  levels of a post-collision fluorine ion in a solid target are transferred from neighboring atoms rather than excited from lower levels of the fluorine ion.

The proposed mechanism for the rapid transfer of electrons to high-lying states of highly ionized fluorine in a solid-state environment involves the depression of the inter-ion potential barrier below the energies of the outermost energy levels of electrons in the neighboring alkali-metal or alkaline-earth ions. This depression of the inter-ion potential barrier occurs as a result of the high positive charge produced at the fluorine site by the heavy-ion collision. As a consequence of the barrier depression, uninhibited electron motion (molecular orbital formation) between neighboring ions becomes possible. A simple classical model calculation indicates that the barrier depression condition is satisfied for  $q$  of the order of 3 or higher and predicts that the levels of the fluorine ion which match most closely the energies of the outer  $np$  levels of the adjacent metal ions are those for  $n=3$  and 4, in excellent agreement with the experimental deductions.

## ACKNOWLEDGMENTS

The help of T. Ritter with the Hartree-Fock calculations and R. Maurer with the experiments is gratefully acknowledged. We thank F. Folkmann for providing us with a copy of the Dirac-Fock program. This work was supported by the U.S. Department of Energy, Office of Basic Energy Sciences, Division of Chemical Sciences, the Robert A. Welch Foundation, and the Texas A&M Center for Energy and Mineral Resources.

\*Present address: Institut für Experimental Physik, Johannes-Kepler-Universität Linz, Linz, Austria.

†Present address: Department of Nuclear Physics, Andhra University, Viskhapatnam 530003, India.

<sup>1</sup>O. Benka, R. L. Watson, and R. A. Kenefick, Phys. Rev. Lett. **47**, 1202 (1981).

<sup>2</sup>O. Benka, R. L. Watson, K. Parthasaradhi, J. M. Sanders, and R. J. Maurer, Phys. Rev. A **27**, 149 (1983).

<sup>3</sup>O. Benka and R. L. Watson, Phys. Lett. **94A**, 143 (1983).

<sup>4</sup>O. Benka, R. L. Watson, and B. Bandong, Phys. Rev. A **28**, 3334 (1983).

<sup>5</sup>R. L. Watson, O. Benka, K. Parthasaradhi, R. J. Maurer, and



- J. M. Sanders, *J. Phys. B* **16**, 835 (1983).
- <sup>6</sup>R. Mann, F. Folkmann, and H. F. Beyer, *J. Phys. B* **14**, 1161 (1981).
- <sup>7</sup>J. A. Bearden, *Rev. Mod. Phys.* **39**, 78 (1967).
- <sup>8</sup>J. P. Desclaux, *Comput. Phys. Commun.* **2**, 31 (1975).
- <sup>9</sup>J. D. Garcia and J. E. Mack, *J. Opt. Soc. Am.* **55**, 654 (1965).
- <sup>10</sup>G. W. F. Drake, *Phys. Rev. A* **19**, 1387 (1979).
- <sup>11</sup>C. F. Fischer, *Comput. Phys. Commun.* **1**, 151 (1969).
- <sup>12</sup>J. C. Slater, *Phys. Rev.* **36**, 57 (1930).
- <sup>13</sup>H. A. Bethe and E. E. Salpeter, *Quantum Mechanics of One and Two Electron Atoms* (Springer, Berlin, 1957).
- <sup>14</sup>O. Benka and R. L. Watson, *Phys. Rev. A* (to be published).
- <sup>15</sup>C. E. Moore, *Atomic Energy Levels as Derived from Analyses of Optical Spectra*, Natl. Bur. Stand. (U.S.) Circ. No. 467 (U.S. GPO, Washington, D.C., 1949), Vol. I.
- <sup>16</sup>M. P. Tosi, in *Solid State Physics*, edited by H. Ehrenreich, F. Seitz, and D. Turnbull (Academic, New York, 1964), Vol. 16, p. 1.
- <sup>17</sup>R. T. Poole, J. Szajman, R. C. G. Leckez, J. G. Jenkins, and J. Liesgang, *Phys. Rev. B* **12**, 5872 (1975).